DECONVOLUTION OF COMPLEX G PROTEIN-COUPLED RECEPTOR SIGNALING IN LIVE CELLS: TAKING ADVANTAGE OF THE RESOLVING POWER OF DYNAMIC MASS REDISTRIBUTION TECHNOLOGY

Ralf Schröder[1], Nicole Janssen[2], Johannes Schmidt[1], Anna Kebig[2], Nicole Merten[1], Stephanie Hennen[1], Anke Müller[1], Stefanie Blättermann[1], Marion Mohr-Andrä[2], Sabine Zahn[3], Jörg Wenzel[3], Nicola J. Smith[4], Jesús Gomeza[1], Christel Drewke[1], Graeme Milligan[4], Klaus Mohr[2], and Evi Kostenis[1]

[1]Molecular-, Cellular-, and Pharmacobiology Section, Institute of Pharmaceutical Biology, University of Bonn, Nussallee 6, 53115 Bonn, Germany

[2]Pharmacology and Toxicology Section, Institute of Pharmacy, University of Bonn, Gerhard-Domagk-Str. 3, 53347 Bonn, Germany

[3]Department of Dermatology, University of Bonn, Sigmund Freud Str. 25, 53105 Bonn, Germany

[4]Molecular Pharmacology Group, Neuroscience and Molecular Pharmacology, Faculty of Biomedical and Life Sciences, University of Glasgow, University Avenue, Glasgow G12 8QQ, Scotland, UK

Corresponding authors: Evi Kostenis

Molecular-, Cellular-, and Pharmacobiology Section

Institute of Pharmaceutical Biology

University of Bonn, 53115 Bonn, Germany

Phone: +49 228 732678/ 733194

Fax: +49 228 733250

Email: kostenis@uni-bonn.de

Klaus Mohr

Pharmacology and Toxicology Section

Institute of Pharmacy

University of Bonn, 53347 Bonn, Germany

Phone: +49 228 73 9103

Fax: +49 228 73 9215

Email: k.mohr@uni-bonn.de

R.S. and N.J. contributed equally to this work.

Short summary

A novel technology platform to deduce signaling of G protein-coupled receptors from cellular dynamic mass redistribution (DMR) is presented and compared with traditional methods used to assess receptor activity. DMR captures signaling through all four major G protein pathways in living cells label-free and in real time, and allows dissection of and new insight into the complex and adaptable signaling biology of recombinant and primary cells with unprecedented accuracy and sensitivity.

Abstract

Dynamic mass redistribution (DMR) represents a novel, label-free, biosensor technology promising to translate GPCR signaling into complex optical "fingerprints" in real time and living cells. Herein, we present a strategy to frame cellular mechanisms that define label-free responses and compare DMR technology with traditional second messenger assays currently state of the art in GPCR drug discovery. The resolving power of DMR enabled us to (1) probe GPCR functionality along all four G protein signaling pathways – at present beyond reach by many other traditional GPCR assay platforms, (2) dissect complex GPCR signaling patterns even in primary human cells with unprecedented accuracy, (3) define heterotrimeric G proteins as the upstream trigger orchestrating the complex optical response profiles, and (4) disclose previously undetected features of GPCR behavior. Significant impact of DMR is therefore anticipated in the emerging areas of systems biology and systems pharmacology but also for the discovery of mechanistically novel drugs.

INTRODUCTION

G protein-coupled receptors (GPCRs) are among the the most important drug target classes[1]. For many members of this receptor family it is now well established that they oscillate among multiple conformations which can be differentially stabilized by ligands thus permitting access to only a subset of the complete repertoire of receptor behaviors[2-8]. This phenomenon, also referred to as biased agonism, functional selectivity or signal trafficking, has an important impact on GPCR drug discovery because it raises the possibility to design signaling pathway-specific therapeutics. Activation of downstream signaling events of GPCRs is traditionally recorded with assays based on quantification of distinct intracellular second messengers such as Ca^{2+}, IP1 and cyclic AMP[5,9-11] and/or translocation of β-arrestin proteins[5,12-16]. Since GPCRs from different coupling classes typically produce one or more specific second messenger, and may additionally engage non-G protein effectors[17-21], several assays are needed to obtain quantitative information about each signaling event. Given the spectrum of cellular activities a single receptor may possess and the dependence of efficacy on the signaling effectors ("pluridimensionality of efficacy"[18]), the need to analyze integrated cellular responses rather than individual components of signaling pathways is becoming increasingly apparent. Dynamic mass redistribution (DMR) is addressed by a novel optical biosensor technology competent to monitor such integrated GPCR signaling responses by detecting redistribution of intracellular constituents triggered upon receptor activation (**Fig. 1a**)[5,22,23]. This method allows quantification of GPCR function in living cells without labeling by capturing receptor activity as optical trace that reflects a generic response of entire living cells reminiscent of holistic responses obtained in tissue or organ bath experiments. Label-free technologies could therefore be decisively advantageous to monitor even complex signaling processes particularly in primary cells which are difficult to analyze with traditional biochemical methods or which are challenging to be transfected with labeled components of

the GPCR signaling cascade for optical studies[23-25]. It is likely that these obstacles have so far precluded assessment of drug candidates in their native environment.

Whereas label-free recording of DMR is already being applied in pharmaceutical companies on a more empirical basis to assess feasibility for high throughput screening, for recording of signaling in immortalized cell lines, or for pharmacological ligand profiling[25-29], no in-depth analytical study is available to date that examines this technology platform and compares it with the methods traditionally used in early drug discovery.

Therefore, we applied DMR to monitor signaling of a variety of GPCRs from different coupling classes in intact living cells and compared the receptor's functionality for inducing a whole cell response with the more classical biochemical approaches to define GPCR signal transduction. An experimental strategy is presented that serves to identify the upstream post-receptor trigger underlying the optical response profiles and thereby allows - in a cell-type specific fashion - to precisely assign optical traces to distinct GPCR-mediated signaling pathways. We then take advantage of this strategy to explore complex GPCR signaling patterns and the mechanism of drug action in both recombinant and primary human cells. Importantly, evidence is provided that only simultaneous visualization of signaling pathways by DMR, but not recording of defined downstream signaling events in single component functional assays, enables identification of unexpected signaling phenomena, thus implying the need to shift from single component to system analysis. We suggest that optical recording of DMR represents an enabling technology with significant impact on both, dissection of complex biological signaling patterns of GPCRs in basic research and understanding of mechanisms of drug action in GPCR drug discovery.

RESULTS

Dynamic mass redistribution faithfully reports signaling of Gi/o-, Gs-, and Gq-linked receptors. CHO cells stably transfected to express the Gi/o-sensitive muscarinic M_2, the Gq-

linked muscarinic M_3, or the Gs-sensitive adrenergic β_2 receptor were challenged with increasing concentrations of their respective agonists, and dynamic mass redistribution (DMR) was recorded as a function of receptor activity. For all three receptors real time optical signatures were concentration-dependent and differed characteristically depending on the primary signaling pathway of each receptor (**Fig. 1b,c,d**). Optical traces required presence of the respective GPCRs since ligand activity was undetectable in native CHO cells (**Supplementary Fig. 1**). To unequivocally characterize whether heterotrimeric G proteins are responsible for orchestrating the specific temporal response patterns, we chose to pharmacologically silence the three G protein signaling pathways using pertussis toxin (PTX) to block Gi/o-, YM-254890 (hereafter referred to as YM) to suppress Gq-[30], and cholera toxin (CTX) to mask Gs-signaling. Indeed, M_2 receptor optical traces were completely abrogated by PTX but unaffected by YM and CTX (**Fig. 1e**) identifying Gi/o proteins as upstream trigger for this optical fingerprint. On their own, these tools did not induce a DMR response (**Supplementary Fig. 2**). Furthermore, G protein-activation as reflected by GTPγS binding assays is in good agreement with DMR data (**Fig. 1h**), thus supporting the notion that the optical traces result from activation of a receptor-dependent Gi-mediated signaling event. Corresponding observations were made for Gs- and Gq-DMR assays: the Gs signatures of the β_2 receptor were exclusively masked by CTX but not by PTX or YM (**Fig. 1f**). The Gq signatures of the M_3 receptor were blunted by YM but not by PTX or CTX (**Fig. 1g** and **Supplementary Fig. 3**); note the enhancement of M_3 signature after pre-treatment with CTX that will be addressed below. Again, traditional second messenger assays suggested that optical traces are a consequence of engaging the respective signaling pathways assigned to both receptors (**Fig. 1i,j**).

Dynamic mass redistribution is competent to identify signaling along the G12/13 pathway. Whereas second messenger assays are well suited to detect activation of Gi-, Gs- and Gq-sensitive receptors, no such assay is yet available to detect G12/13 signaling apart

from high content screening or those approaches that assume contribution of these G proteins by recording mostly far removed downstream events[31]. Here it is demonstrated that DMR provides information about signaling through this fourth Gα protein family. We took advantage of the recently deorphanized atypical cannabinoid receptor GPR55 which represents the only GPCR known to date with exclusive bias towards the G12/G13 pathway[8,32,33]. Human embryonic kidney (HEK293) cells, which were virtually unresponsive in DMR assays to lysophosphatidylinositol (LPI) - at present the most suitable GPR55 agonist[32-34] - (**Supplementary Fig. 4a**) were chosen to establish a stable GPR55-expressing clone. Of note, wild-type CHO cells responded with robust DMR signals to LPI challenge, while the same cells did not show any significant LPI-effect in traditional second messenger assays covering the Gi-, Gs-, and Gq pathways and were therefore judged unsuitable for transfection with and functional exploration of GPR55 (**Supplementary Fig. 4b-d**). GPR55-HEK cells displayed concentration-dependent optical traces upon exposure to LPI (**Fig. 2a**,**b**). Interestingly, GPR55-mediated DMR was insensitive to PTX, CTX and YM but silenced when cells were pretreated with the pan-G protein activator aluminiumfluoride AlF_4^- (AlF) (**Fig. 2c**). AlF_4^- treatment of cells completely occluded GPR55 activity but did not cause a general lack of responsiveness of these cells in DMR assays due to an elevated DMR baseline (**Supplementary Fig. 5**). These data suggest G protein origin of the GPR55 trace but absence of coupling to Gi/o, Gs and Gq proteins, a conclusion which is further corroborated by the lack of second messenger production in GPR55-HEK cells (**Supplementary Fig. 6**). Importantly, GPR555-HEK cells transfected to coexpress dominant negative G13 (G13dn, G13Q226L,D294N) did not display altered GPR55 cell surface expression (**Supplementary Fig. 7**) but significantly diminished LPI-induced DMR responses, whereas – for control - optical traces elicited by carbachol acting through endogenously expressed Gq-sensitive muscarinic receptors were virtually unaffected (**Fig. 2d-f**). Hence, DMR is competent to visualize signaling along the G12/13 pathway and therefore represents a methodology

applicable to probe functionality of GPCRs from all four coupling classes which at present is beyond reach by most other GPCR assay platforms.

Dynamic mass redistribution response profiles are cell type-dependent. Since signaling-dependent relocation of cellular constituents is likely to depend on the cellular background, Gi-, Gs-, and Gq-triggered DMR responses were also examined in HEK293 cells. The Gi/o-coupled CRTH2 receptor unveiled a signature profile with significant similarity to that observed for the Gi-coupled M_2 receptor in CHO cells (**Fig. 3a**, compare **Fig. 1b**). Remarkably similar DMR traces were also obtained when a panel of additional Gi/o-coupled receptors including the 5-oxo-ETE receptor (OXER), the nicotinic acid receptor HM74A, and the free fatty acid receptor FFA3 (**Supplementary Fig. 8**) were analyzed supporting the notion that optical traces may indeed be suggestive for engagement of particular signaling pathways. However, activation of the Gs signaling cascade in HEK cells achieved with the lipid mediator prostaglandin E_1 (PGE_1) acting via the two endogenously expressed Gs-linked EP2/EP4 receptors or with orciprenaline stimulating endogenous β_2 receptors gave rise to positive DMR in contrast to the downward-deflected Gs signature in CHO cells (**Fig. 3f** and **Supplementary Fig. 9**, compare **Fig. 1c**). Reminiscent cellular context dependency was also observed when forskolin, a direct adenylyl cyclase activator that bypasses the receptor was applied. DMR responses of forskolin are essentially superimposable to those induced by stimulation of Gs GPCR agonists in both CHO and HEK293 cells (**Supplementary Fig. 10**). Apparently, unique differences exist in the spatiotemporal organization of the Gs-downstream signaling network in these two cell lines. Again, differentiation of signatures with pathway modulators (**Fig. 3b-d,g-i**), specific receptor antagonists (data not shown), and second messenger assays (**Fig. 3e,j**) confirmed and validated that optical traces for the tested Gi- and Gs-sensitive receptors faithfully reflect stimulation of signaling pathways previously assigned to these receptors.

Simultaneous recording of multiple cellular signaling events uncovers signaling promiscuity. FFA1 has previously been classified as Gq/11-sensitive receptor[35-37]. Stimulation of FFA1-HEK cells with the small molecule agonist TUG424[38] induced robust DMR responses, distinct in shape from those obtained for Gi- and Gs-coupled receptors in this cellular background (compare **Fig. 4a** with **Fig. 3a,f**). However, unlike expected for a Gq-sensitive receptor, FFA1-mediated DMR was only partly sensitive to inhibition by YM (**Fig. 4b**, compare black and blue trace), although the same concentration of YM was sufficient to completely silence FFA1-dependent Gq/11 activity in IP1 assays (**Fig. 4c**). Apparently, FFA1 is not restricted to the Gq/11 pathway in this particular cellular background but engages an additional signaling route. Indeed, FFA1 also activates Gi/o, inferred from partial PTX sensitivity of the DMR signal (**Fig. 4b** compare black and grey trace) and a PTX-sensitive component in ERK1/2 MAP kinase phosphorylation assays (**Supplementary Fig. 11**). In agreement with a dual Gq-Gi coupling profile, only the combination of PTX and YM was required and sufficient to completely erase the FFA1 response (**Fig. 4b**, compare black and red trace). Strikingly, however Gi activity of FFA1 was hardly detectable when inhibition of forskolin-stimulated cAMP production was measured in parallel second messenger assays (**Fig. 4d**) which is well in agreement with previous observations[35,36]. These findings highlight the strength of DMR technology: not only does DMR offer access to high content integrated cellular information, it also provides mechanistic insight if combined with the inhibitor strategy proposed herein to deconvolute complex signaling pathways.

Dynamic mass redistribution allows analysis of GPCR functionality in human primary cells. Analyzing GPCR-mediated signal transduction in primary human cells, i.e. the cell type in which medicines are intended to mediate their therapeutic effect, is highly desirable for GPCR drug candidates. To test whether DMR is sufficiently sensitive to detect GPCR signaling in a native environment, we chose the cAMP-elevating agent PGE_1 as a stimulus, known to affect cell growth and cytokine production of human keratinocytes[39], and monitored

DMR in both immortalized (HaCaT cells) and primary human keratinocytes obtained from six patients that underwent skin surgery. HaCaT and primary human keratinocytes responded with concentration-dependent optical traces reminiscent of those already observed in PGE_1-treated EP2/EP4-HEK293 cells (**Fig. 5a,b**, compare **Fig. 3f**). Indeed, PGE_1 traces in both HaCaT and primary human keratinocytes reflect activation of the two Gs-coupled EP2 and EP4 receptors since the responses were sensitive to inhibition by a combination of EP2 and EP4 antagonists (**Fig. 5c,d**) – which when applied alone hardly diminished PGE_1 traces (data not shown, n=3) -, and invisible following CTX- but not PTX- or YM-treatment (**Fig. 5e,f** and data not shown). Note: although cAMP and DMR assays were both sufficiently sensitive to quantify PGE_1 activity in primary human cells, DMR was significantly superior with respect to quality of the signal window under conditions of low receptor expression in human primary cells (**Fig. 5g,h**).

Dynamic mass redistribution uncovers unknown signaling paradigms. It has been shown previously that persistent activation of the Gs signaling pathway can augment muscarinic M_3 receptor-mediated inositol phosphate production[40]. At first glance, the results reported herein might appear to be in good accordance with this earlier report as we detected enhanced muscarinic M_3 receptor signaling in the presence of cAMP elevating agents such as CTX (**Fig. 1g** and **Fig. 6a**) and forskolin (**Fig. 6b**; red versus black trace). Surprisingly, however, these enhanced M_3 signaling responses in DMR assays were sensitive to pre-treatment of the cells with PTX implying a Gi/o-mediated event (**Fig. 6a,b**; red versus blue trace). In contrast, M_3 DMR was completely insensitive to PTX pre-treatment when intracellular cAMP was not elevated prior to application of the muscarinic agonist (**Fig. 6a,b**; grey versus black trace). Apparently, elevated intracellular cAMP – when present prior to the muscarinic agonist – serves as a stimulus to confer onto the M_3 receptor the ability to engage an additional signaling pathway. Importantly, detection of Gi activity under conditions of elevated cAMP can also be accomplished by immunocapture GTPγS binding assays (**Fig. 6c**) but not

traditional cAMP inhibition assays, where receptor agonist and forskolin need to be co-applied simultaneously but not sequentially to obtain measurable cAMP level changes as exemplified for the bona fide Gi linked muscarinic M_2 receptor (**Supplementary Fig. 12**).

DISCUSSION

GPCRs constitute the single largest family of cell surface receptors attracting great interest as therapeutic targets in all major disease areas[1]. Accordingly, assay technologies enabling discovery of novel GPCR ligands impact the drug discovery process greatly. Recently, label-free technology platforms based on dynamic mass redistribution of intracellular proteins (Corning® Epic® Biosensor, for operating principle see **Fig. 1a**) or alteration of electric impedance have emerged for the study of GPCRs[5,22-25,41]. Although it is frequently claimed that label-free assays may hold great promise for GPCR drug discovery[5], no in-depth analytical study is available to date that has thoroughly validated the novel DMR technology and/or compared it with the more traditional biochemical and second messenger assays which have been the mainstay in GPCR drug development.

Our results show that DMR technology is unique in that it captures receptor activation of all four GPCR coupling classes (Gi/o, Gs, Gq, G12/13) which at present is unachievable by most other technology platforms. It therefore represents a truly universal, pathway-unbiased yet pathway-sensitive approach towards investigation of G protein-mediated effects. Capability to detect signaling along the G12/13 pathway may be of great relevance to future deorphanization strategies, particularly as receptors previously considered to be non-signaling might exclusively signal through G12/13. Although lack of pathway-bias is a great advantage for deorphanization studies, the possibility must be considered that DMR traces- if opposing in direction and possessing identical kinetics – may yield zero signatures and therefore mask activity of biologically relevant molecules. Nevertheless, the use of pathway blockers would disclose hidden pathway activation.

DMR technology- and traditional second messenger assay-platforms also deviate greatly in another aspect: DMR displays an overall cellular response, most likely encompassing a variety of cellular events downstream of the GPCR[5,22-24] which is in stark contrast to quantification of defined second messengers that only contribute to the overall cellular response. In addition, the total cellular level of a second messenger may not necessarily reflect its local concentration at a site of strategic importance within a signaling cascade. These aspects are likely to explain why agonist potencies determined with both methods may, but do not necessarily have to converge. Indeed, the present study revealed an at least equal or even superior sensitivity (**Fig. 1i**) of DMR- as compared with second messenger-recording for the detection of receptor-dependent, G protein-mediated signaling.

Complexity of optical traces obviously raises the possibility that an unimaginable wealth of intracellular players may be involved in defining the fine details of signature amplitude and duration. It will be exciting to unravel the individual components shaping complex optical response patterns. Utilization of libraries of signaling pathway inhibitors could be a starting point, genome-wide genetic screens exploring siRNA libraries yet another. Our study does not solve the signature riddle completely but provides a major mechanistic advance towards understanding the complex optical traces: heterotrimeric G proteins represent the postreceptor trigger responsible for orchestrating the complex response profiles for the various receptors and cellular backgrounds examined herein, which was demonstrated using a combination of toxins and pharmacological pathway inhibitors.

The experimental power of these tools in label-free detection has been shown in this study for many different receptors and various cellular backgrounds including primary human keratinocytes Given the emerging successes in directing differentiation of embryonic or pluripotent stem cells to mature cells such as neurons or endothelial cells[42,43], label-free DMR detection opens the exciting perspective to expand mechanism of drug action studies and even drug screening processes to physiologically relevant cells. Native signaling has already been

addressed in publications using label-free DMR detection[25]. All of these reports, however, have embarked on analysis of immortalized cell lines[25] which are much less close to tissue biology as compared with primary human cells used herein.

Another striking revelation of this study is how the collation of signaling routes within one dynamic all-encompassing response and its mechanistic deconvolution with appropriate pharmacological tools visualizes both expected and unexpected signaling phenomena. Identification of an additional signaling pathway for the free fatty acid FFA1 receptor is such an example. In fact, application of DMR technology to disclose ligand efficacy along the Gi pathway is particularly noteworthy since this aspect of FFA1 behavior is hardly detectable in the traditional cAMP inhibition assay (**Fig. 4d**). Yet another example is constituted by identification of cAMP as intracellular stimulus to increase the signaling repertoire of the muscarinic M3 receptor. Although M3-Gi interaction has been inferred indirectly based on partial PTX-sensitivity of M3-mediated responses many years ago[44,45], a defined stimulus for this event has remained elusive so far. It is therefore important to stress that this particular mode of cellular crosstalk has been uncovered for two reasons: (i) because DMR visualizes the summation of individual GPCR signaling routes during a single experiment, and (ii) because DMR – in contrast to traditional biochemical assays - does not require pharmacological manipulation of the second messenger adenylyl cyclase-cAMP pathway to probe G protein (Gi) activity.

In summary, comparative analysis of traditional biochemical methods with the novel DMR technology platform uncovers the experimental power of whole-cell label-free detection: not only does DMR provide a temporally resolved readout for the summation of receptor-triggered signaling events in recombinant and primary living cells with unprecedented sensitivity and accuracy, it is this cumulative readout of cellular activity which opens the exciting perspective to disclose further levels of biological complexity in the regulation of signal transduction processes. We therefore anticipate that DMR as a holistic read-out of cell

function will advance the emerging areas of systems biology and systems pharmacology and thereby promote the discovery of mechanistically novel therapeutics.

ACKNOWLEDGEMENTS

We thank Ulrike Rick and Marianne Vasmer-Ehses for expert technical assistance and Corning® Inc. for providing us with the Epic® system. This work was supported by the DFG (Deutsche Forschungsgemeinschaft) grants KO 1582/3-1 to E.K., MO 821/2-1 to K.M. and WE 4428/1-1 to J.W. and the Dr. Hilmer foundation (PhD fellowship to S.H.). A.K. is member of the Research Training School GRK 677, which is supported by the DFG. We thank Marco De Amici and Ulrike Holzgrabe (University of Milan, Italy, and University of Würzburg, Germany) for kindly providing Hybrid 1[46], Trond Ulven (University of Southern Denmark) for TUG424[38] and Astellas Pharma Inc. (Osaka, Japan) for providing us with YM-254890[30].

AUTHOR CONTRIBUTIONS

R.S., N.J., J.S., A.K., S.H., A.M., S.B., N.M., M.M.A., N.J.S., designed and performed the experiments, E.K. and K.M. designed research and wrote the manuscript, S.Z., J.W., G.M. provided important biological samples or research tools, C.D., J.G., and R.S. provided important ideas and edited the manuscript.

DISCLOSURES

The authors declare no competing financial interests.

FIGURE LEGENDS

Figure 1: Dynamic mass redistribution enables analysis of differential receptor-mediated G protein activation in CHO cells.

(**a**) Sketch of the Epic® technique for real-time measurement of dynamic mass redistribution (DMR). Traditional second messenger assays are included.

?: conventional second messenger assay is not known. For details see text and Methods section.

(**b-j**) Shown are recordings in CHO cells stably transfected with either the hM_2-, $h\beta_2$-, or hM_3-receptor gene (left, middle, right panel, respectively).

(**b-d**) The cell lines were challenged with the indicated concentrations of the corresponding agonist (M_2: hybrid 1, β_2: orciprenaline, M_3: acetylcholine) and wave length shift was monitored as a measure of receptor activation. Representative data (mean + s.e.m.) of at least four independent experiments.

(**e-g**) Validation by toxin-pretreatment of agonist-induced Gi-, Gs-, and Gq activation: pertussis toxin 100 ng/ml (PTX), cholera toxin 100 ng/ml (CTX), YM 254890 300 nM (YM). Representative data (mean + s.e.m.) from at least three independent experiments. Control 1 corresponds to YM signature, control 2 corresponds to PTX and CTX signatures.

(**h-j**) Comparison of concentration-effect-curves resulting from DMR assays and traditional assays. Calculated log EC_{50} values are: (**h**) M_2 DMR: -7.21 $\pm$ 0.27, GTPγS: -7.63 $\pm$ 0.07; (**i**) β_2 DMR: -8.35 $\pm$ 0.24, cAMP: -7.34 $\pm$ 0.03; (**j**) M_3 DMR: -6.99 $\pm$ 0.20, IP1: -7.1 $\pm$ 0.07. All data are means ($\pm$ s.e.m) of at least three independent experiments.

Figure 2: Dynamic mass redistribution visualizes signaling along the G12/13 pathway.

(**a**) GPR55-HEK cells were challenged with the indicated concentrations of the GPR55 agonist lysophosphatidylinositol (LPI) and wavelength shift was monitored over time as a measure of receptor activation. Data shown are representative (mean + s.e.m.) of at least three independent experiments.

(**b**) Concentration-effect curve for LPI in GPR55-HEK cells resulting from DMR traces in three independent experiments. The calculated log EC_{50} value is -7.34 $\pm$ 0.05.

(**c**) LPI-mediated alteration of cell activity in GPR55-HEK cells is not blunted by pre-treatment with toxin (5 ng/ml PTX, 100 ng/ml CTX) or pathway inhibitor (300 nM YM-254890), but is sensitive to pre-incubation of cells with 300 µM of the pan-G protein agonist AlF_4^- (AlF). Shown are representative data (mean + s.e.m.) from at least three independent experiments.

(**d**,**e**,**f**) LPI- but not carbachol-mediated DMR is significantly diminished in GPR55-HEK cells cotransfected to express a dominant negative form of G13 (G13dn, G13Q226L,D294N). GPR55 cells cotransfected to express G13dn or empty pcDNA3.1 vector DNA were treated with 1 µM LPI (**d**) or 100 µM carbachol (**e**) and DMR was monitored over time. Depicted are representative optical traces (**d**,**e**) and concentration effect relationships of five such experiments (**f**).

Figure 3: Dynamic mass redistribution enables measurement of differential receptor-mediated G protein activation in HEK293 cells.

Shown are DMR and second messenger assays performed with the following cell lines and receptors: (**a-e**) HEK293 cells stably expressing CRTH2, (**f-j**) HEK293 cells endogenously expressing EP2/EP4 receptors.

(**a**,**f**) Cells were challenged with the indicated concentrations of agonists and wavelength shift was monitored as a measure of receptor activation. Shown are representative data (mean + s.e.m.) of at least three independent experiments.

(**b**,**g**) Pre-treatment of cells with 5 ng/ml PTX inhibits signaling of the Gi-sensitive CRTH2 receptor but not signaling of the Gs-sensitive EP2/EP4 receptors.

(**c**,**h**) Pre-treatment of cells with 100 ng/ml CTX (or 10 µM forskolin) masks signaling of the Gs-sensitive EP2/EP4 receptors but does not affect Gi traces of CRTH2.

(**d**,**i**) Pre-treatment of cells with 300 nM YM does not alter CRTH2 or EP2/EP4 traces. All data are normalized to the maximum response obtained in the absence of pharmacological inhibitors.

(**e**,**j**) Comparison of DMR assays with traditional cAMP second messenger assays. (**e**) CRTH2-mediated decrease of intracellular cAMP is calculated as percent inhibition of adenylyl cyclase stimulated with 10 µM forskolin. Calculated log EC_{50} values are: DMR: -7.96 $\pm$ 0.04, cAMP: -7.85 $\pm$ 0.34; (**j**) EP2/EP4-mediated responses in DMR and cAMP assays are normalized to the maximum responses obtained by 10 µM PGE_1 in each assay. Calculated log EC_{50} values are: DMR: -8.11 $\pm$ 0.07, cAMP: -8.11 $\pm$ 0.12. All data are means ($\pm$ s.e.m.) of at least three independent experiments.

Figure 4: **Parallel visualization of all signaling pathways unveils an additional signaling route of the free fatty acid receptor FFA1.**

(**a**) DMR recordings of FFA1-HEK cells treated with the indicated concentrations of the small molecule agonist TUG424[38].

(**b**) The DMR signature obtained with 3 µM of the small molecule FFA1 agonist TUG424 is partly sensitive to pre-treatment of FFA1-HEK cells with PTX (5 ng/ml) or YM (300 nM) but completely abrogated in the presence of a combination of PTX and YM.

(**c**) FFA1-mediated production of the second messenger IP1 is completely blunted in the presence of 300 nM YM. FFA1-HEK cells were stimulated with 3 µM TUG424 and the resulting accumulation of inositol phosphates (IP1) was detected with an HTRF®-IP1 assay kit as described in the Methods section.

(**d**) FFA1-activation of the Gi signaling pathway is hardly detectable but significant in cAMP inhibition assays. FFA1-HEK - or HEK293 cells for control - were stimulated

with 5 µM forskolin and inhibition of cAMP formation was quantified with an HTRF®-cAMP assay kit as outlined in the Methods section. The cAMP level induced by stimulation with 5 µM forskolin (Fsk) was set 100 %. Shown are mean values and s.e.m. of three to six independent experiments. For statistical analysis, individual concentrations were compared by two-way ANOVA with Bonferroni's correction for multiple comparisons. **p<0.01, ***p<0.001.

Figure 5: Dynamic mass redistribution enables analysis of GPCR functionality in immortalized and primary human keratinocytes.

Left panels: immortalized human keratinocytes (HaCaTs), right panels: primary human keratinocytes. (**a**,**b**) The cell lines were challenged with the indicated concentrations of PGE_1 and wavelength shift over time was monitored as a measure of receptor activation. (**a**) Representative data (+ s.e.m.) of at least four independent experiments. (**b**) Representative data (+ s.e.m.) of cells from one human donor. Cells of five additional human donors yielded comparable optical traces (not shown).

(**c**,**d**) PGE_1-mediated DMR is inhibited by pre-treatment with a combination of the EP2 and EP4 receptor antagonists AH6809 and L161,982 respectively. Optical traces of 30 nM PGE_1 (**c**) or 100 nM PGE_1 (**d**) in the absence and presence of a combination of 10 µM AH6809 and 3 µM L161,982. All data are representative data (+ s.e.m.) of at least four independent experiments.

(**e**,**f**) DMR signatures of 100 nM PGE_1 are masked when cells are pretreated with 250 ng/ml cholera toxin (CTX). (**e**) Representative data (+ s.e.m.) of at least four independent experiments. (**f**) One representative data set (+ s.e.m.) from one out of five human subjects.

(**g**,**h**) Comparison of DMR assays with traditional endpoint cAMP second messenger assays. Calculated log EC_{50} values are: (**g**) HaCaT: DMR: -8.27 ± 0.09, cAMP: -7.78

± 0.09; (**h**) keratinocytes: DMR: -7.70 ± 0.06, cAMP: -7.60 ± 0.12. All data are means (± s.e.m.) of at least four independent experiments.

Figure 6: The muscarinic M_3-receptor adapts to adenylyl cyclase activation with a changed signaling repertoire. Set of DMR experiments addressing (**a**) indirect and (**b**) direct activation of adenylyl cyclase by CTX and forskolin (Fsk), respectively. Acetylcholine (100 µM)-induced DMR traces were measured under control conditions and after pre-treatment with pertussis toxin 100 ng/ml (PTX), cholera toxin 100 ng/ml (CTX), or forskolin 10 µM as indicated. Representative data (mean + s.e.m.) from at least three independent experiments. Note that PTX sensitivity emerges only after pre-treatment with either CTX or forskolin. (**c**) GTPγS binding assay on membranes prepared from M_3-CHO cells. M_3-CHO cells were grown to confluence and left untreated or were pre-treated with cholera toxin (20 h, 100 ng/ml) prior to membrane preparation. GTPγS incorporation was determined in the absence and presence of 1 mM acetylcholine followed by immuno-enrichment of Gi proteins with an antiserum to the C terminal region common to Gi proteins, as described in the Methods section (mean + s.e.m., n= 3). P values less than 0.05 were considered statistically significant according to one-way analysis of variance (ANOVA) with Bonferroni's correction for multiple comparisons, as appropriate.

MATERIALS AND METHODS

Materials and reagents:

Tissue culture media reagents were from Invitrogen (Karlsruhe, Germany) or Sigma-Aldrich (Taufkirchen, Germany). Prostaglandin E_1 (PGE_1), 13,14-dihydro-15-keto-prostaglandin D_2 ($DK\text{-}PGD_2$) and AH6809 from Cayman (Ann Arbor, MI, USA), L161,982 from Tocris (Bristol, UK) forskolin (Fsk) from Applichem (Darmstadt, Germany) and [^{35}S]GTPγS from Perkin Elmer (Rodgau - Jügesheim, Germany). All other chemicals were obtained from Sigma-Aldrich (Taufkirchen, Germany) unless explicitly indicated.

Cell culture and cell lines stably expressing individual GPCRs:

The following receptors (human sequences) and cell lines were used: Flp-In^{TM}-Chinese hamster ovary cells (Flp-In^{TM}-CHO) stably expressing the M_2 or the M_3 receptor referred herein as M_2-CHO and M_3-CHO, CHO cells stably expressing the GPR55 or the β_2 receptor (GPR55-CHO and β_2-CHO) and untransfected CHO cells. CHO cells were cultured in Ham´s nutrient mixture F-12 (HAM-F12) supplemented with 10 % (v/v) fetal calf serum (FCS), 100 U/ml penicillin, 100 µg/ml streptomycin. The medium was complemented with 2 mM glutamine for M_2-CHO and M_3-CHO, 1 mM L-glutamine and 200 µg/ml G418 for β_2-CHO and 400 µg/ml G418 for GPR55-CHO.

HEK293 cells and HEK293 cells stably expressing CRTH2 (CRTH2-HEK cells), HEK293-Flp-In^{TM} T-REx^{TM} cells stably transfected with FFA1 (FFA1-HEK) and AD-HEK293 stably transfected with 3xHA-GPR55 (GPR55-HEK, kindly provided by Andrew Irving, University of Dundee, UK) were cultured in Dulbecco´s modified Eagle´s medium (DMEM) supplemented with 10 % (v/v) FCS, 100 U/ml penicillin and 100 µg/ml streptomycin. For CRTH2-HEK and GPR55-HEK the medium was supplemented with 500 µg/ml G418, and for FFA1-HEK with 100 µg/ml hygromycin B and 15 µg/ml blasticidin (both: InvivoGen,

Toulouse, France). For receptor expression FFA1-HEK cells were treated with 1 µg/ml doxycyclin for 16 h.

Immortalized keratinocytes (HaCaT, human adult low calcium temperature) were grown in RPMI-1640 supplemented with 10 % (v/v) FCS, 100 U/ml penicillin and 100 µg/ml streptomycin.

Primary human keratinocytes were obtained from skin samples of healthy patients and were cultured in KGM2 (Promocell, Heidelberg, Germany) supplemented with 100 U/ml penicillin and 100 µg/ml streptomycin. All patients had written an informed consent before excision. The study was approved by the local ethic committee (concession-no. 090/04).

All cells were cultivated with 5% CO_2 at 37°C.

Transient transfections of GPR55-HEK cells:

To effectively deliver cDNA coding for dominant-negative G13 (G13Q226L,D294N) into GPR55-HEK cells an electroporation method was used described previously[47]. DMR measurements were performed 48 h after transfection.

Dynamic mass redistribution (DMR) assays (Corning® Epic® Biosensor measurements):

A beta version of the Corning® Epic® System was used consisting of a temperature-control unit, an optical detection unit, and an on-board robotic liquid handling device. Principle: A confluent cell layer adheres to the bottom of a well equipped with an optical biosensor. Ingoing broadband light is directed to travel along the bottom. The electromagnetic field extends into the cell layer for a depth of about 150 nm, loses energy depending on the optical density of the adjacent cell area and outgoing wavelength is measured. GPCR-mediated signaling affects optical density and thereby shifts outgoing wavelength (pm) relative to pre-stimulus condition and is recorded over time. The magnitude of this wavelength shift is

proportional to the amount of relocated intracellular matters: increase of mass contributes positively and decrease negatively to the overall response[22,23].

Cells were seeded onto 384-well Epic® sensor microplates and cultured for 20-24 h to obtain confluent monolayers. GPR55 cells were treated as described previously[34].
Prior to the assay cells were washed with assay-buffer (HBSS with 20 mM HEPES) and transferred to the Epic® reader for 2 h at 28°C. DMR was monitored before and after addition of compound solutions. The incubation time for pre-treatment with PTX or CTX was 16-20 h, for YM-254890 2.5 h, for aluminiumfluoride 1.5 h, and for forskolin 1-2.5 h.

[^{35}S]GTPγS assay:

Membranes were prepared from M2-CHO cells and [^{35}S]GTPγS incorporation measured as described previously[48]. For muscarinic M3 receptors [^{35}S]GTPγS binding assays included an immuno-capture step with an antiserum to the C-terminus of Gi and were performed according to a previously published procedure[49]

Second messenger accumulation assays (over expressed receptors):

cAMP and IP1 accumulation was quantified with the HTRF®-cAMP dynamic kit or the HTRF®-IP1 kit, respectively (both Cisbio, Bagnols-sur-Cèze Cedex, France) as per manufacturer's instructions and as described previously[50] on a Mithras LB 940 reader (Berthold Technologies, Bad Wildbad, Germany).

cAMP accumulation assay (endogenously expressed receptors): cAMP accumulation was quantified with the competitive immunoassay HitHunter™ cAMP-HS+-kit (DiscoveRx Corporation, Fremont, USA) as per manufacturer's instructions using the Mithras LB 940 reader.

Calculations and Data Analysis:

Quantification of DMR signals for concentration effect curves was performed either by calculation of the area under the curve (AUC) between 0 and 3600 s (**Fig. 1i,j, Fig. 2b,f, Fig. 3j**, **Fig. 5g**,**h**) or by the maximum value between 300 and 1200 s (**Fig. 1h**, **Fig. 3e**) for those traces that displayed fast kinetics and clear peak maxima. All optical DMR recordings were buffer/solvent-corrected. For data normalization, indicated as relative response (%), top levels of concentration effect curves were set 100 % and bottom levels 0 %. Data calculation and EC_{50} value determination by nonlinear regression was performed using Prism 4.02 (Graph Pad, San Diego, CA, USA).

Statistical Analysis:

Where appropriate, differences in means were examined by one-way analysis of variance (ANOVA) with Bonferroni's multiple comparison post-hoc test using GraphPad Prism 5.01 (GraphPad Software, San Diego, CA, USA). A p value < 0.05 was considered statistically significant.

References

1. Overington, J.P., Al-Lazikani, B. & Hopkins, A.L. How many drug targets are there? *Nat. Rev. Drug Discov.* **5**, 993-996 (2006).
2. Baker, J.G. & Hill, S.J. Multiple GPCR conformations and signalling pathways: implications for antagonist affinity estimates. *Trends Pharmacol. Sci.* **28**, 374-381 (2007).
3. Bosier, B. & Hermans, E. Versatility of GPCR recognition by drugs: from biological implications to therapeutic relevance. *Trends Pharmacol. Sci.* **28**, 438-446 (2007).
4. Galandrin, S., Oligny-Longpre, G. & Bouvier, M. The evasive nature of drug efficacy: implications for drug discovery. *Trends Pharmacol. Sci.* **28**, 423-430 (2007).
5. Kenakin, T.P. Cellular assays as portals to seven-transmembrane receptor-based drug discovery. *Nat. Rev. Drug. Discov.* **8**, 617-626 (2009).
6. Urban, J.D. et al. Functional selectivity and classical concepts of quantitative pharmacology. *J. Pharmacol. Exp. Ther.* **320**, 1-13 (2007).
7. Kenakin, T. Agonist-receptor efficacy. II. Agonist trafficking of receptor signals. *Trends Pharmacol. Sci.* **16**, 232-238 (1995).
8. Ryberg, E. et al. The orphan receptor GPR55 is a novel cannabinoid receptor. *Br. J. Pharmacol.* **152**, 1092-1101 (2007).
9. Eglen, R.M. Functional G protein-coupled receptor assays for primary and secondary screening. *Comb. Chem. High Throughput Screen.* **8**, 311-318 (2005).
10. Williams, C. cAMP detection methods in HTS: selecting the best from the rest. *Nat. Rev. Drug. Discov.* **3**, 125-135 (2004).
11. Willoughby, D. & Cooper, D.M. Live-cell imaging of cAMP dynamics. *Nat. Methods* **5**, 29-36 (2008).
12. Barnea, G. et al. The genetic design of signaling cascades to record receptor activation. *Proc. Natl. Acad. Sci. U S A* **105**, 64-69 (2008).
13. Hamdan, F.F., Audet, M., Garneau, P., Pelletier, J. & Bouvier, M. High-throughput screening of G protein-coupled receptor antagonists using a bioluminescence resonance energy transfer 1-based beta-arrestin2 recruitment assay. *J. Biomol. Screen.* **10**, 463-475 (2005).
14. Lefkowitz, R.J. & Whalen, E.J. beta-arrestins: traffic cops of cell signaling. *Curr. Opin. Cell. Biol.* **16**, 162-168 (2004).
15. Olson, K.R. & Eglen, R.M. Beta galactosidase complementation: a cell-based luminescent assay platform for drug discovery. *Assay Drug Dev. Technol.* **5**, 137-144 (2007).
16. Verkaar, F. et al. G protein-independent cell-based assays for drug discovery on seven-transmembrane receptors. *Biotechnol Annu Rev* **14**, 253-274 (2008).
17. Azzi, M. et al. Beta-arrestin-mediated activation of MAPK by inverse agonists reveals distinct active conformations for G protein-coupled receptors. *Proc. Natl. Acad. Sci. U S A* **100**, 11406-11411 (2003).
18. Galandrin, S. & Bouvier, M. Distinct signaling profiles of beta1 and beta2 adrenergic receptor ligands toward adenylyl cyclase and mitogen-activated protein kinase reveals the pluridimensionality of efficacy. *Mol. Pharmacol.* **70**, 1575-1584 (2006).
19. Hansen, J.L., Theilade, J., Haunso, S. & Sheikh, S.P. Oligomerization of wild type and nonfunctional mutant angiotensin II type I receptors inhibits galphaq

protein signaling but not ERK activation. *J. Biol. Chem.* **279**, 24108-24115 (2004).
20. Hoffmann, C., Ziegler, N., Reiner, S., Krasel, C. & Lohse, M.J. Agonist-selective, receptor-specific interaction of human P2Y receptors with beta-arrestin-1 and -2. *J. Biol. Chem.* **283**, 30933-30941 (2008).
21. Violin, J.D. & Lefkowitz, R.J. Beta-arrestin-biased ligands at seven-transmembrane receptors. *Trends Pharmacol. Sci.* **28**, 416-422 (2007).
22. Fang, Y., Ferrie, A.M., Fontaine, N.H., Mauro, J. & Balakrishnan, J. Resonant waveguide grating biosensor for living cell sensing. *Biophys. J.* **91**, 1925-1940 (2006).
23. Fang, Y., Li, G. & Ferrie, A.M. Non-invasive optical biosensor for assaying endogenous G protein-coupled receptors in adherent cells. *J. Pharmacol. Toxicol. Methods* **55**, 314-322 (2007).
24. Fang, Y. & Ferrie, A.M. Optical biosensor differentiates signaling of endogenous PAR1 and PAR2 in A431 cells. *BMC Cell Biol.* **8**, 24 (2007).
25. Rocheville, M. & Jerman, J.C. 7TM pharmacology measured by label-free: a holistic approach to cell signalling. *Curr. Opin. Pharmacol.* **9**, 643-649 (2009).
26. Dodgson, K., Gedge, L., Murray, D.C. & Coldwell, M. A 100K well screen for a muscarinic receptor using the Epic label-free system--a reflection on the benefits of the label-free approach to screening seven-transmembrane receptors. *J. Recept. Signal Transduct. Res.* **29**, 163-172 (2009).
27. Lee, P.H. et al. Evaluation of dynamic mass redistribution technology for pharmacological studies of recombinant and endogenously expressed g protein-coupled receptors. *Assay Drug Dev. Technol.* **6**, 83-94 (2008).
28. McGuinness, R.P. et al. Enhanced selectivity screening of GPCR ligands using a label-free cell based assay technology. *Comb. Chem. High Throughput Screen.* **12**, 812-823 (2009).
29. Peters, M.F., Vaillancourt, F., Heroux, M., Valiquette, M. & Scott, C.W. Comparing Label-Free Biosensors for Pharmacological Screening With Cell-Based Functional Assays. *Assay Drug Dev. Technol.* (in press).
30. Takasaki, J. et al. A novel Galphaq/11-selective inhibitor. *J. Biol. Chem.* **279**, 47438-47445 (2004).
31. Riobo, N.A. & Manning, D.R. Receptors coupled to heterotrimeric G proteins of the G12 family. *Trends Pharmacol. Sci.* **26**, 146-154 (2005).
32. Henstridge, C.M. et al. The GPR55 ligand L-alpha-lysophosphatidylinositol promotes RhoA-dependent Ca2+ signaling and NFAT activation. *Faseb J.* **23**, 183-193 (2009).
33. Ross, R.A. The enigmatic pharmacology of GPR55. *Trends Pharmacol. Sci.* **30**, 156-163 (2009).
34. Henstridge, C.M. et al. GPR55 ligands promote receptor coupling to multiple signalling pathways. *Br. J. Pharmacol.* (in press).
35. Briscoe, C.P. et al. The orphan G protein-coupled receptor GPR40 is activated by medium and long chain fatty acids. *J. Biol. Chem.* **278**, 11303-11311 (2003).
36. Itoh, Y. et al. Free fatty acids regulate insulin secretion from pancreatic beta cells through GPR40. *Nature* **422**, 173-176 (2003).
37. Stoddart, L.A., Brown, A.J. & Milligan, G. Uncovering the pharmacology of the G protein-coupled receptor GPR40: high apparent constitutive activity in guanosine 5'-O-(3-[35S]thio)triphosphate binding studies reflects binding of an endogenous agonist. *Mol. Pharmacol.* **71**, 994-1005 (2007).

38. Christiansen, E. et al. Discovery of potent and selective agonists for the free fatty acid receptor 1 (FFA(1)/GPR40), a potential target for the treatment of type II diabetes. *J. Med. Chem.* **51**, 7061-7064 (2008).
39. Zhang, J.Z., Maruyama, K., Iwatsuki, K., Ono, I. & Kaneko, F. Effects of prostaglandin E1 on human keratinocytes and dermal fibroblasts: a possible mechanism for the healing of skin ulcers. *Exp. Dermatol.* **3**, 164-170 (1994).
40. McGraw, D.W., Almoosa, K.F., Paul, R.J., Kobilka, B.K. & Liggett, S.B. Antithetic regulation by beta-adrenergic receptors of Gq receptor signaling via phospholipase C underlies the airway beta-agonist paradox. *J. Clin. Invest.* **112**, 619-626 (2003).
41. McGuinness, R. Impedance-based cellular assay technologies: recent advances, future promise. *Curr. Opin. Pharmacol.* **7**, 535-540 (2007).
42. Gaspard, N. et al. Generation of cortical neurons from mouse embryonic stem cells. *Nature Protoc.* **4**, 1454-1463 (2009).
43. James, D. et al. Expansion and maintenance of human embryonic stem cell-derived endothelial cells by TGFbeta inhibition is Id1 dependent. *Nature Biotechnol.* **28**, 161-166 (2010).
44. Burford, N.T., Tobin, A.B. & Nahorski, S.R. Differential coupling of m1, m2 and m3 muscarinic receptor subtypes to inositol 1,4,5-trisphosphate and adenosine 3',5'-cyclic monophosphate accumulation in Chinese hamster ovary cells. *J. Pharmacol. Exp. Ther.* **274**, 134-142 (1995).
45. Schmidt, M., Nehls, C., Rumenapp, U. & Jakobs, K.H. m3 Muscarinic receptor-induced and Gi-mediated heterologous potentiation of phospholipase C stimulation: role of phosphoinositide synthesis. *Mol. Pharmacol.* **50**, 1038-1046 (1996).
46. Antony, J. et al. Dualsteric GPCR targeting: a novel route to binding and signaling pathway selectivity. *Faseb J.* **23**, 442-450 (2009).
47. Pantaloni, C. et al. Alternative splicing in the N-terminal extracellular domain of the pituitary adenylate cyclase-activating polypeptide (PACAP) receptor modulates receptor selectivity and relative potencies of PACAP-27 and PACAP-38 in phospholipase C activation. *J. Biol. Chem.* **271**, 22146-22151 (1996).
48. Jäger, D. et al. Allosteric small molecules unveil a role of an extracellular E2/transmembrane helix 7 junction for G protein-coupled receptor activation. *J. Biol. Chem.* **282**, 34968-34976 (2007).
49. Smith, N.J., Stoddart, L.A., Devine, N.M., Jenkins, L., Milligan, G. The action and mode of Binding of thiazolidinedione ligands at free fatty acid receptor 1. *J.Biol.Chem.* 284, 17527-17539 (2009)
50. Schröder, R. et al. The C-terminal tail of CRTH2 is a key molecular determinant that constrains Galphai and downstream signaling cascade activation. *J. Biol. Chem.* **284**, 1324-1336 (2009).

Figure 1 (Kostenis)

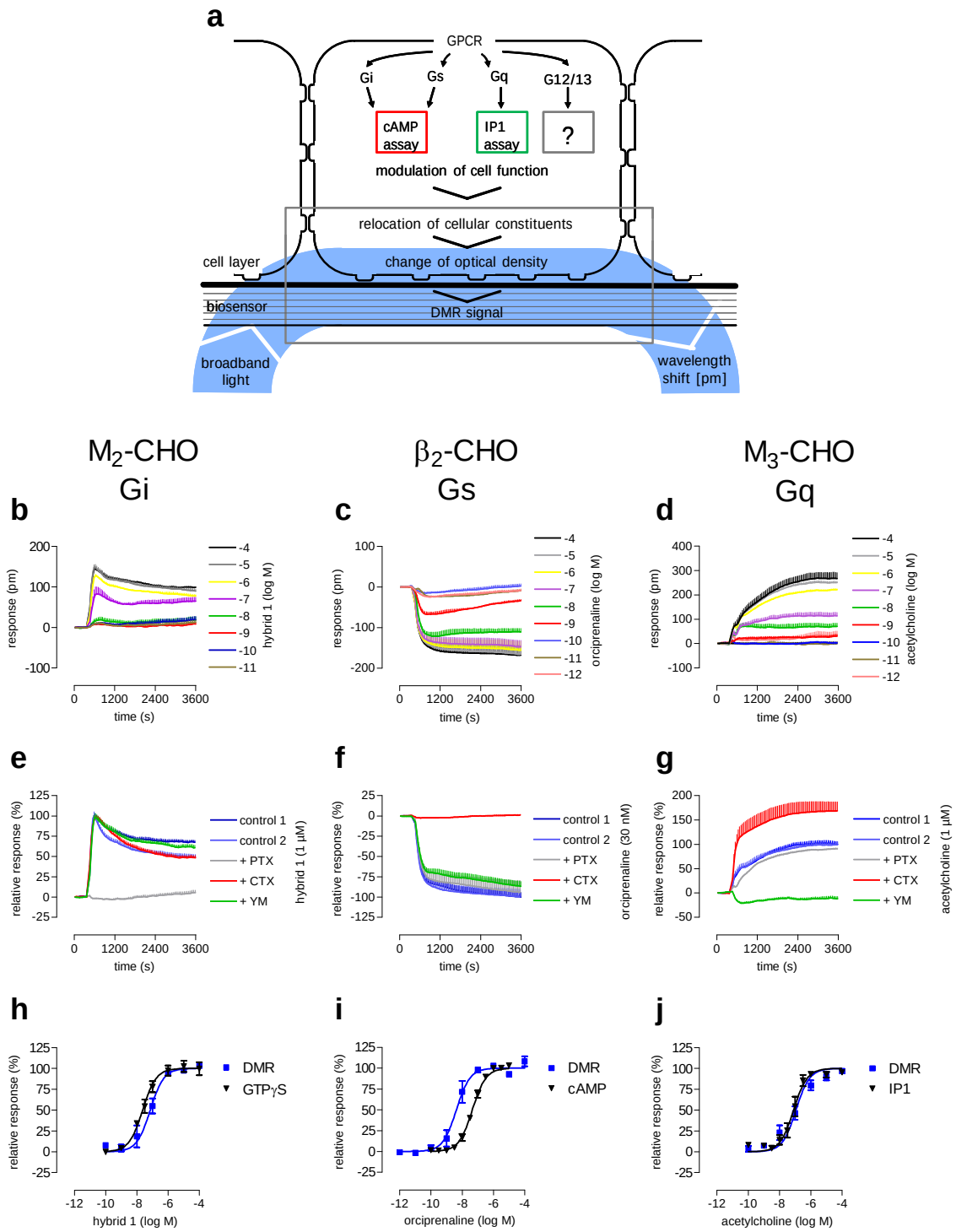

Figure 2 (Kostenis)

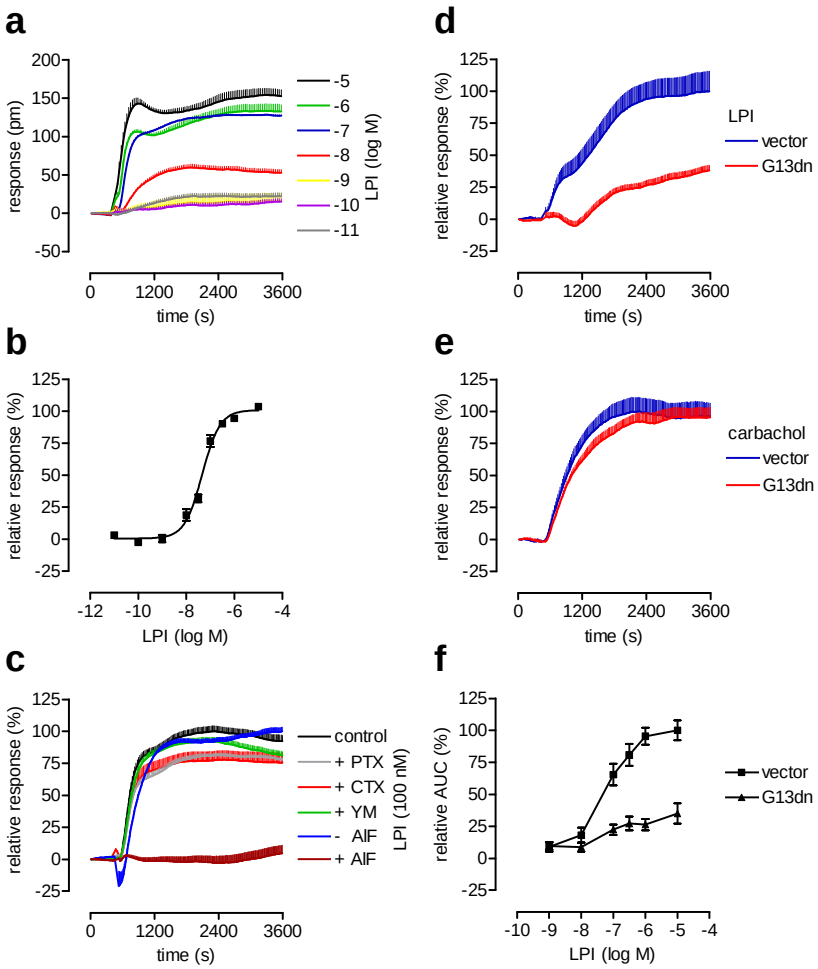

Figure 3 (Kostenis)

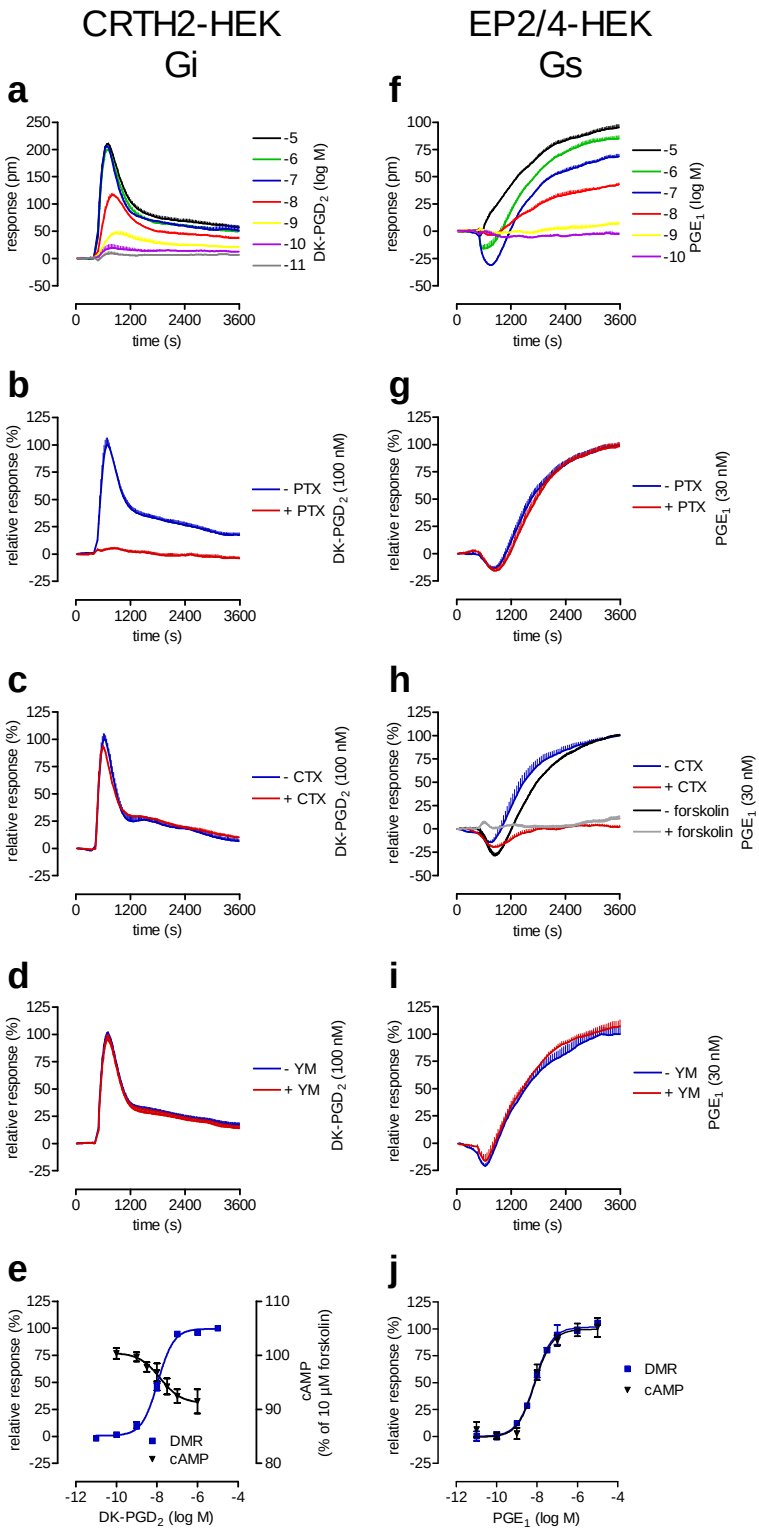

Figure 4 (Kostenis)

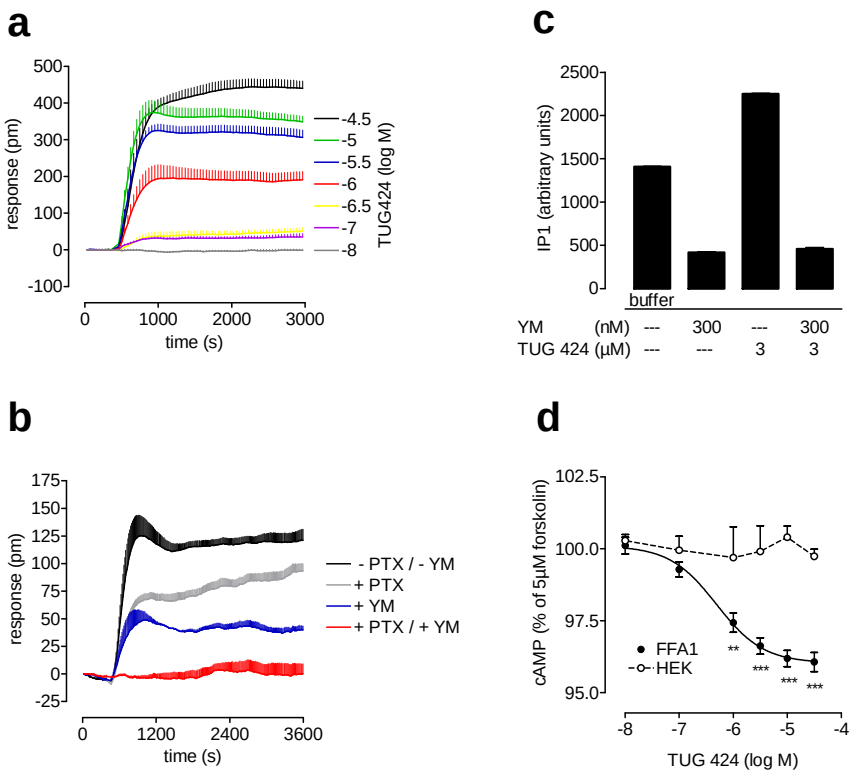

Figure 5 (Kostenis)

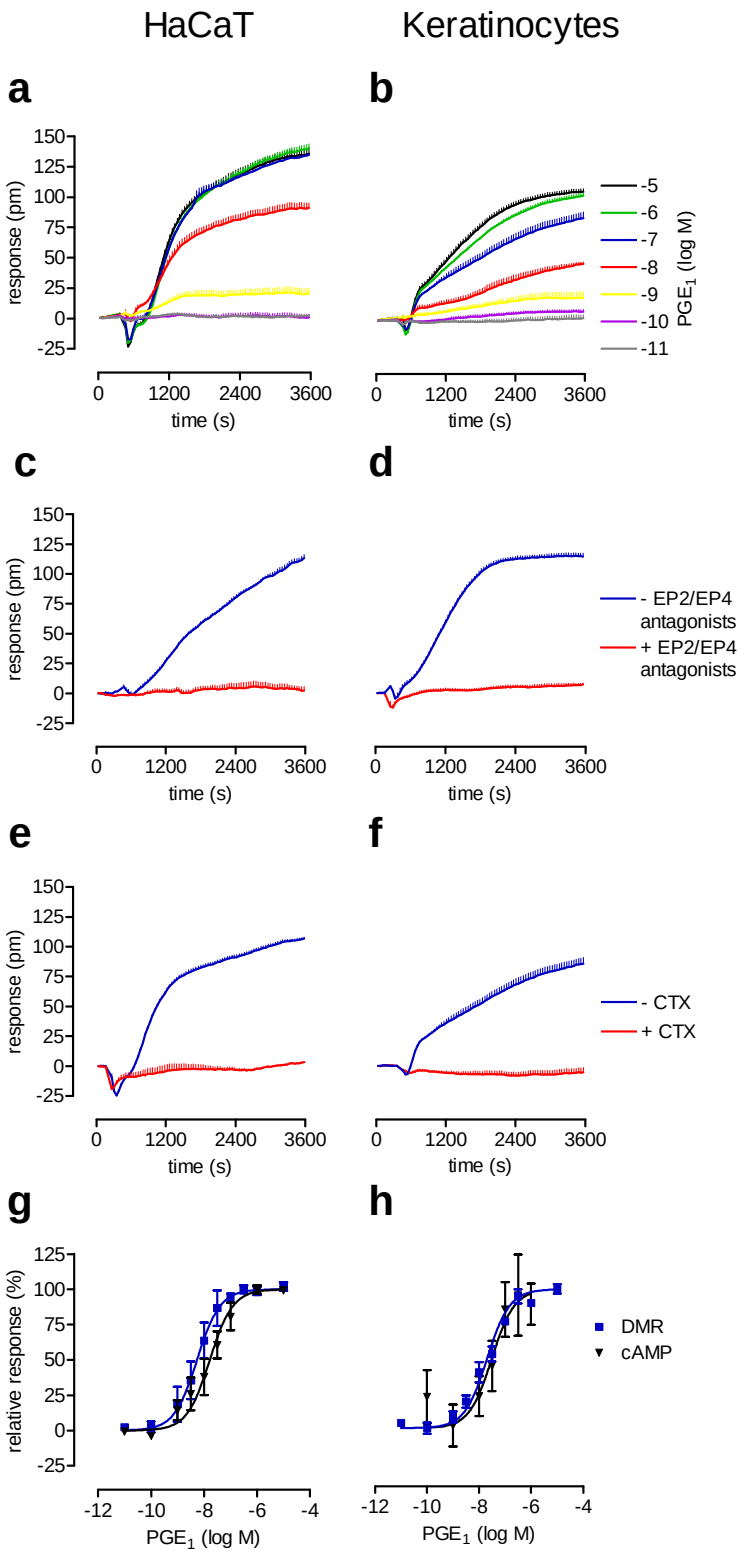

Figure 6 (Kostenis)

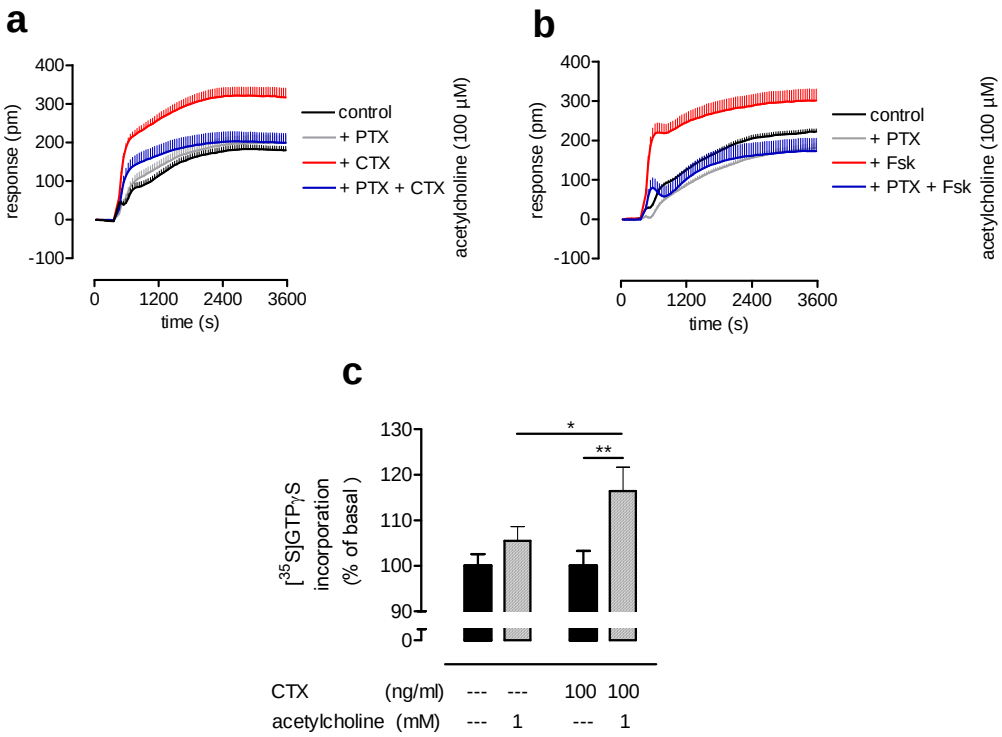

Supplementary Figure 1 (Kostenis)

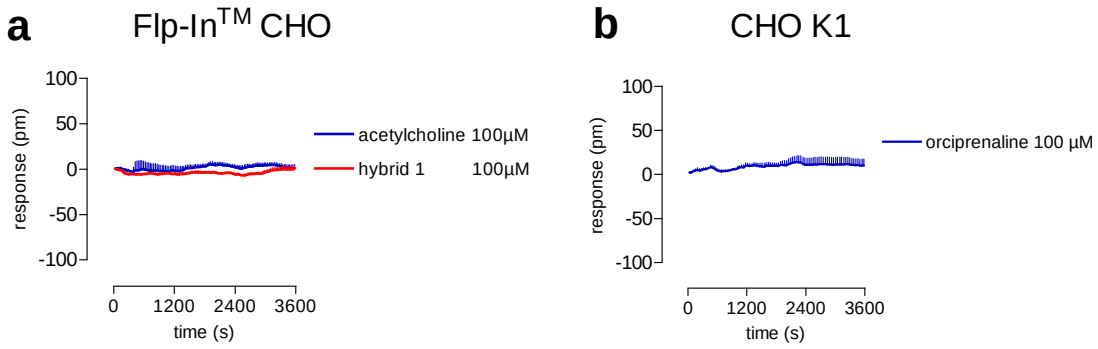

Supplementary Figure 1: Lack of agonist-induced DMR in non-transfected CHO cells.

(a, b) CHO Flp-In™ cells (left panel) or CHO K1 cells (right panel) were exposed to the indicated agonists at maximally effective concentrations and wavelength shift (ordinate) was measured. Shown are data (mean values + s.e.m.) from a representative experiment. Similar findings were obtained in at least two independent additional experiments.

Supplementary Figure 2 (Kostenis)

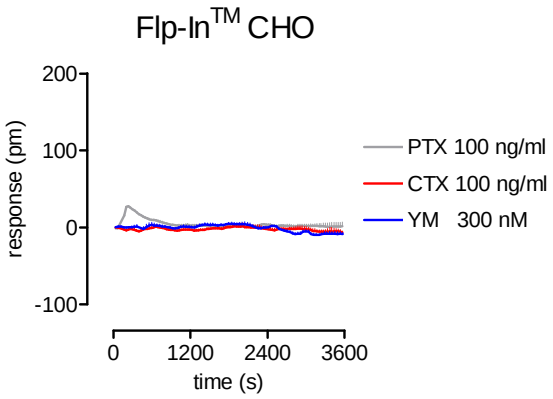

Supplementary Figure 2: The pathway modulators pertussis toxin, cholera toxin and YM-254890 do not induce significant mass redistribution in native CHO cells. Flp-In™ CHO cells were exposed to the indicated concentrations of pathway modulators and wavelength shift was recorded over time. Shown are data (mean values + s.e.m.) from a single experiment representative for at least three such experiments.

Supplementary Figure 3 (Kostenis)

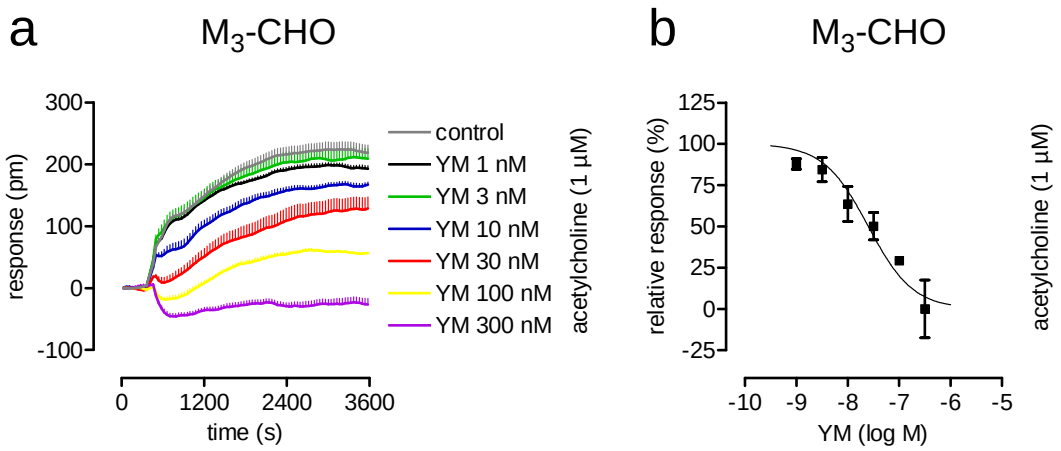

Supplementary Figure 3: Potency and efficacy of the Gq inhibitor YM-254890 to quench the human muscarinic M_3 receptor-mediated DMR-response.

Shown are recordings in CHO cells stably transfected with the human muscarinic M_3 receptor cDNA (M_3-CHO).

(**a**) Cells were pretreated with the indicated concentrations of the Gq inhibitor YM-254890 (YM) and wavelength shift was monitored as a measure of receptor activation by 1 µM acetylcholine. Representative data (mean + s.e.m.) of at least three independent experiments.

(**b**) Concentration-effect-curve resulting from DMR signals at 3600 sec.: log IC_{50} value is: -7.60 ± 0.09 (top, bottom, slope factor fixed to 100%, 0% and -1, respectively).

Supplementary Figure 4 (Kostenis)

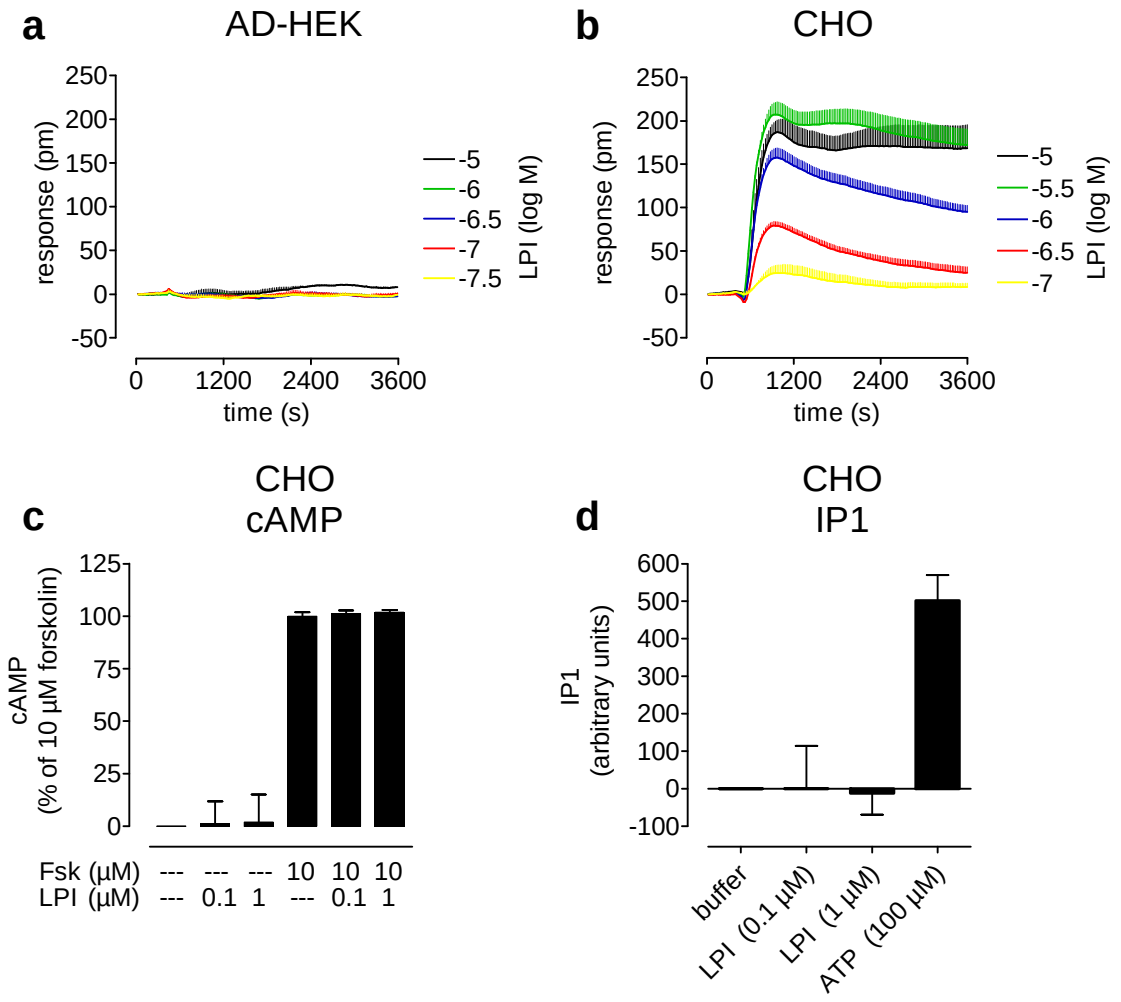

Supplementary Figure 4: Comparison of LPI responsiveness in native HEK293 and CHO cells. Native AD-HEK cells (**a**) or native CHO cells (**b**) were challenged with the indicated concentrations of LPI and wavelength shift over time was monitored as a measure of receptor activation. Depicted are mean values + s.e.m. of optical traces from one experiment, representative for three such experiments.

(**c**) LPI neither increased accumulation of cAMP nor inhibited forskolin-stimulated cAMP production in native CHO cells. cAMP levels were determined with an HTRF® cAMP assay kit as outlined in detail in the Methods section. Data shown are mean values and s.e.m. of three independent experiments.

(**d**) LPI does not mobilize hydrolysis of inositol phosphates in native CHO cells as opposed to the positive control ATP (agonist of endogenous Gq-sensitive nucleotide P2Y receptors). IP1 levels were determined with an HTRF® IP1 assay kit as outlined in detail in the Methods section. Data shown are mean values and s.e.m. of three independent experiments.

Supplementary Figure 5 (Kostenis)

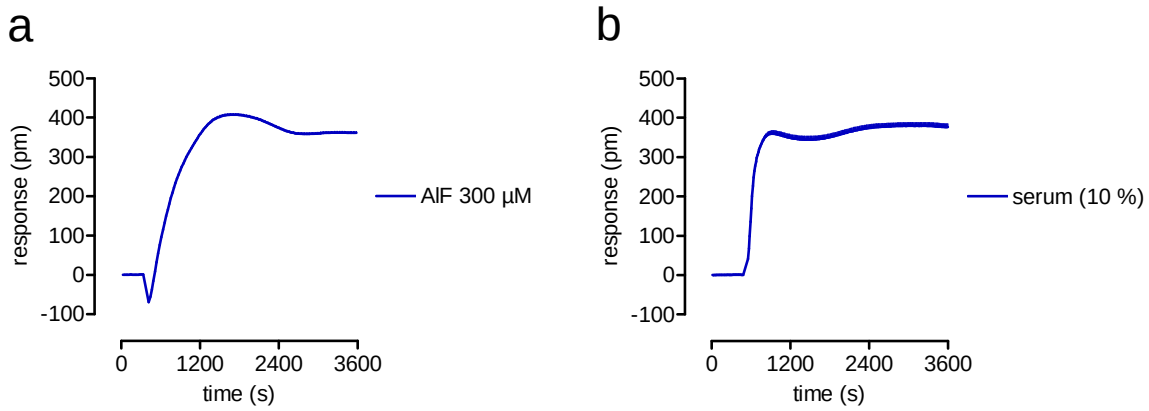

Supplementary Figure 5: Treatment of cells with aluminiumfluoride $AlF4^-$ (AlF) causes robust DMR changes on its own but does not cause general unresponsiveness of cells to DMR stimuli. (**a**) GPR55-HEK cells were exposed to 300 µM of the pan G protein agonist AlF_4^- and the resultant wavelength shift was recorded over time. (**b**) GPR55-HEK cells pretreated for 1.5 h with 300 µM AlF_4^- were challenged with serum to promote growth factor activation. AlF_4^- pretreatment which promotes a robust DMR response on its own, completely silences GPR55 activity (cf Figure 2) but does still allow for additional DMR changes to occur in response to growth factor containing serum. Shown are representative optical traces (mean values + s.e.m.) from a single experiment, representative for at least four such experiments.

Supplementary Figure 6 (Kostenis)

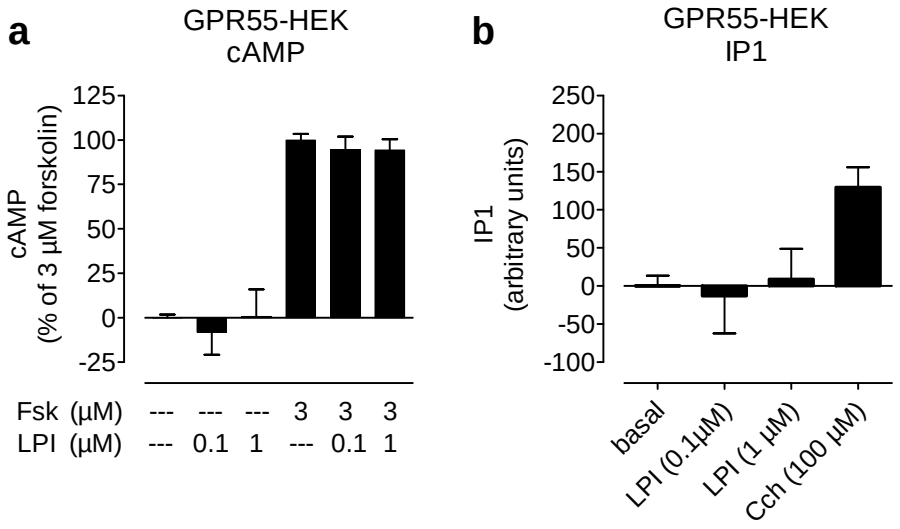

Supplementary Figure 6: LPI does not alter the levels of the second messengers cAMP and IP1 in GPR55-HEK cells.

(**a**) LPI neither increased accumulation of cAMP nor inhibited forskolin-stimulated cAMP production in GPR55-HEK293 cells. cAMP levels were determined with an HTRF® cAMP assay kit as outlined in detail in the Methods section. Data shown are mean values and s.e.m. of three to four independent experiments.

(**b**) GPR55-HEK cells were stimulated with the indicated concentrations of lysophosphatidylinositol (LPI) or carbachol (Cch) as a control (activator of endogenously expressed muscarinic receptors) and the resulting accumulation of IP1 was detected with an HTRF®-IP1 assay kit as described in the Method section.

Supplementary Figure 7 (Kostenis)

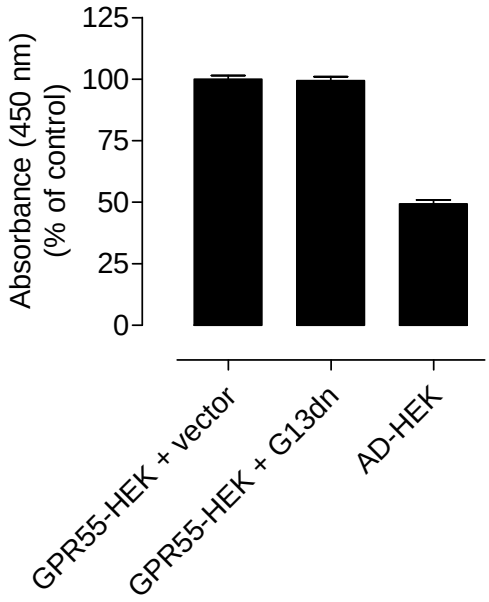

Supplementary Figure 7: Coexpression of G13dn does not impact cell surface expression of GPR55. AD-HEK293 cells stably expressing GPR55 (GPR55-HEK) or not (AD-HEK) were transiently transfected with G13dn or pcDNA3.1 control plasmid and surface expression quantified by ELISA as described in the Method section. Absorbance of GPR55-HEK cells transfected with pcDNA3.1 vector DNA was set 100%. Data shown are mean values + s.e.m. of three independent experiments each performed in triplicate.

Supplementary Figure 8 (Kostenis)

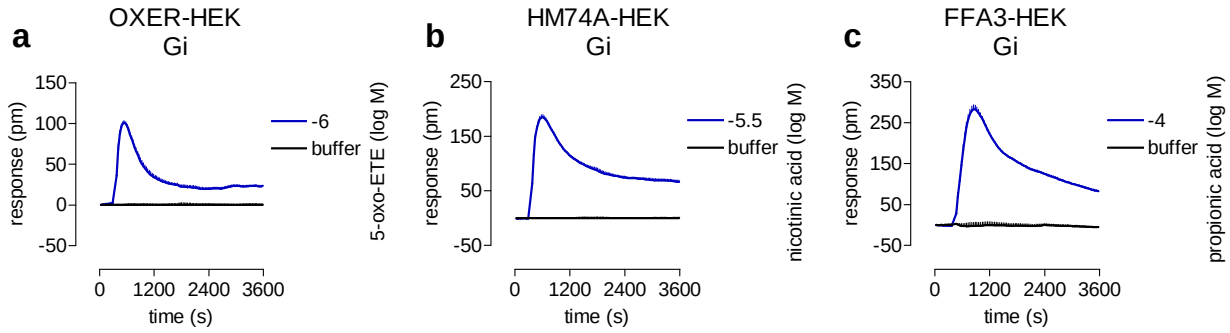

Supplementary Figure 8: Kinetic response profiles of Gi/o-linked G protein-coupled receptors in DMR assays. HEK293 cells transiently transfected to express the Gi/o-coupled 5-oxo-ETE (OXER) receptor (**a**), the nicotinic acid receptor HM74A (**b**), or the short chain fatty acid receptor FFA3 (**c**) were exposed to the indicated concentrations of receptor agonists and wavelength shift over time was monitored as a measure of receptor activation. Depicted are mean values + s.e.m. of optical traces from one experiment, representative for at least three such experiments.

Supplementary Figure 9 (Kostenis)

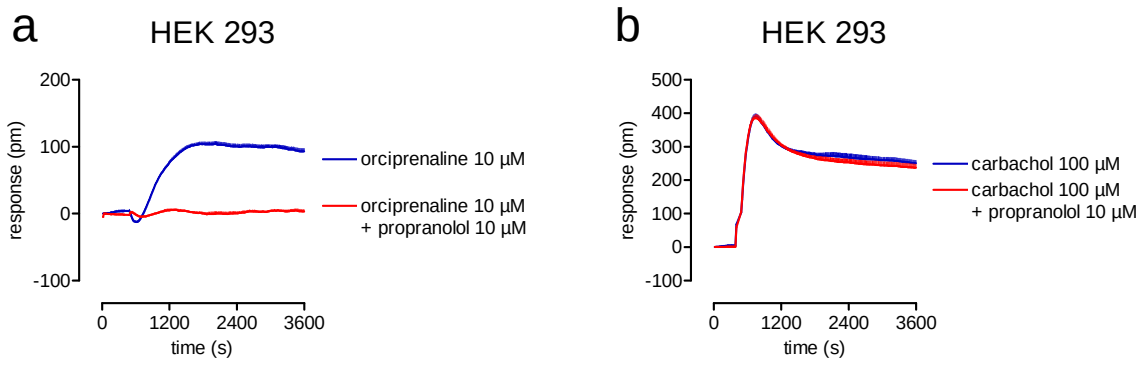

Supplementary Figure 9: Kinetic response profile of the adrenergic β_2 receptor endogenously expressed in HEK293 cells. (**a**) HEK293 cells were exposed to 10 µM of the β_2 agonist orciprenaline and wavelength shift over time was monitored as a measure of receptor activation. The orciprenalin trace can be specifically inhibited by the β receptor antagonist propranolol. (**b**) Propranolol does not diminish the DMR response triggered upon stimulation of endogenous muscarinic receptors with carbachol, confirming its specific inhibitory action. Depicted are mean values + s.e.m. of optical traces from one experiment, representative for four such experiments.

Supplementary Figure 10 (Kostenis)

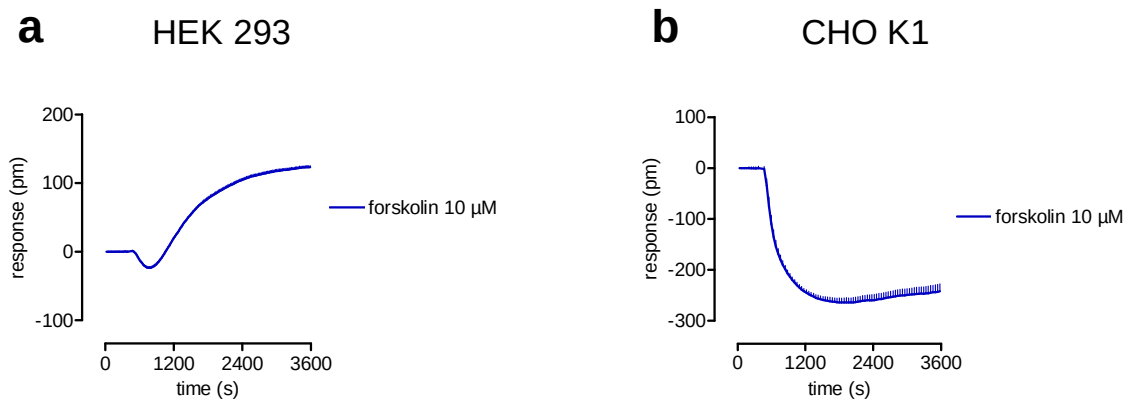

Supplementary Figure 10: DMR response profile of the adenylyl cyclase activator forskolin in HEK293 and CHO cells. HEK293 (**a**) and CHO K1 cells (**b**) cells were exposed to the indicated concentrations of forskolin and wavelength shift over time was monitored as a measure of adenylyl cyclase activation. Depicted are mean values + s.e.m. of optical traces from one experiment, representative for at least six independent experiments.

Supplementary Figure 11 (Kostenis)

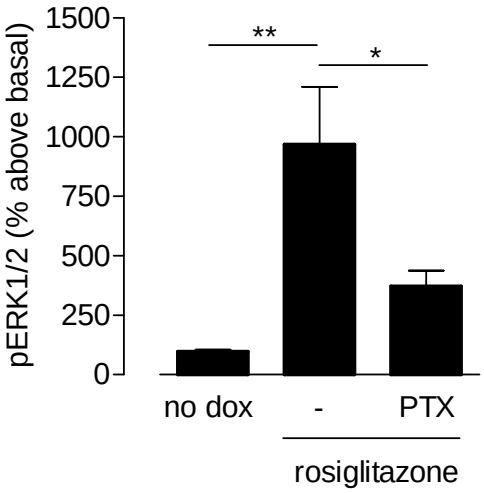

Supplementary Figure 11: FFA1-mediated activation of ERK1/2 phosphorylation involves stimulation of Gi/o proteins. HEK293 Flp-In™ T-REx cells expressing inducible FFA1-eYFP ells were treated with 0.5 µg/ml doxycycline for 48 h to induce receptor expression and ERK1/2 MAP kinase activation was quantified with the SureFire AlphaScreen assay as described in the Method section. For Gi/o inhibition, separate wells were treated with 20ng/ml of pertussis toxin for approximately 16 h. Response to the agonist rosiglitazone (100 µM) was measured after 30 min of stimulation. Shown are mean values + s.e.m. of three independent experiments each performed in duplicates, where doxycycline-induced untreated response was normalized to 100 per cent. *p<0.05, **p<0.01 according to one-way ANOVA with Bonferroni's multiple comparisons test.

Supplementary Figure 12 (Kostenis)

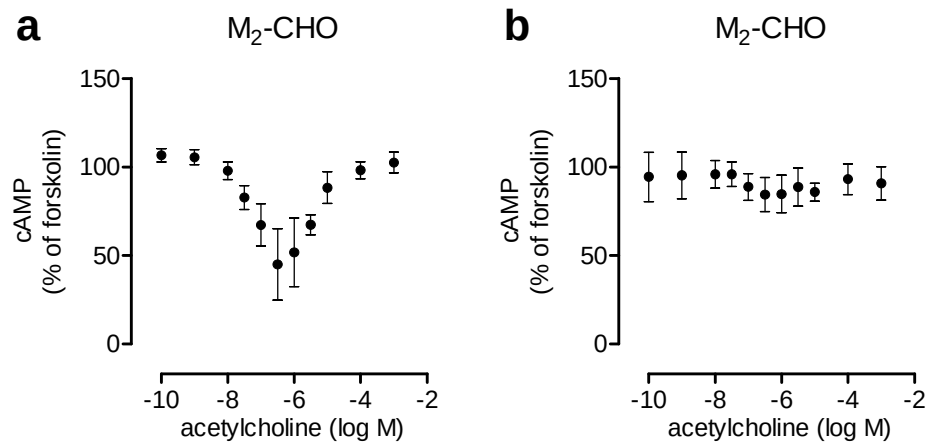

Supplementary Figure 12: Acetylcholine-induced intracellular cAMP shift in M_2-CHO-cells (a) without and (b) with forskolin (10 µM)-pre-treatment for 2 hours. M_2-mediated alteration of intracellular cAMP is calculated as percent inhibition of adenylyl cyclase stimulated with 7.5 µM forskolin (**a**) and 10 µM forskolin (**b**). Note: in (**a**) acetylcholine and forskolin are applied simultaneously, i.e. Gi stimulation can only be observed if adenylyl cyclase activity is enhanced. In (**b**) forskolin was applied 2 hours prior to acetylcholine. Gi activity is hardly detectable under these conditions. Intracellular levels of cAMP were detected with an HTRF®-cAMP assay kit as described in detail in the Method section. Shown are mean values ± s.e.m. of six (**a**) or three (**b**) independent experiments.

MATERIAL AND METHODS SUPPLEMENTARY MATERIAL (KOSTENIS)

Chemicals:

Nicotinic acid and propionic acid were purchased from Sigma-Aldrich (Taufkirchen, Germany) and 5-oxo-6E,8Z,11Z,14Z-eicosatetraenoic acid (5-oxo-ETE) from Cayman (distributed by Biozol, Eching, Germany).

Plasmid origin:

The high-affinity nicotinic acid receptor HM74A[1] was PCR amplified from human adipose tissue cDNA and inserted into the pcDNA3.1(+) expression vector via 5' HindIII and 3'EcoRI sites. The receptor for 5-oxo-eicosatetraenoic acid (OXE) receptor[2] and the FFA3 receptor[3] were cloned from human leukocyte cDNA and inserted via 5′ HindIII and 3′ EcoRI into pcDNA3.1(+). Correctness of the constructs was verified by restriction endonuclease digestion and sequencing in both directions (MWG Biotech, Ebersberg, Germany). 3xHA-GPR55 cDNA was obtained from the UMR cDNA resource center.

Cell culture and transient transfection of HEK293 cells:

HEK293 cells were cultured as described in Material and Methods. 24 h before transfection cells were plated at a density of 4 million cells/10 cm^2 dish. Cells were transfected using a calcium phosphate-DNA co-precipitation method, where 20 µg of cDNA was diluted in 500 µl of $CaCl_2$ solution (10 mM Tris base, 1 mM EDTA, pH 8, and 250 mM $CaCl_2$) and dropwise added to 500 µl of HBS (280 mM NaCl, 50 mM HEPES, and 1.5 mM sodium phosphate). The precipitation was incubated for 45 min at room temperature and was added to the cells in 10 ml of fresh culture medium and was incubated at 37°C in a 5% CO_2-humidified atmosphere, 5 h later medium was changed. One day after transfection, the cells were transferred to fibronectin coated Epic® 384 microwell plates at a density of 15.000 cells/well and cultured in growth media for additional 18-24 h. Cells were then subjected to functional analysis using dynamic mass redistribution (DMR) as described in Material and Methods.

Cell culture of CHO K1 and CHO Flp-In™ cells

CHO cell lines were cultured in Ham´s nutrient mixture F-12 (HAM-F12) (Sigma, Taufkirchen, Germany) supplemented with 10 % (v/v) fetal calf serum (FCS), 100 U/ml penicillin, 100 µg/ml streptomycin, and 1mM L-glutamine.

ELISA

Determination of cell-surface expression levels of GPR55 containing an N-terminal triple HA-tag was performed in stable GPR55-HEK293 cells transiently cotransfected to express either G13dn or pcDNA3.1 control plasmid. Twenty-four hours after transfection, cells were seeded in poly-D-lysine-coated 48-well tissue-culture plates at a density of 50,000 cells/well. Approximately 48 h after transfection, cells were washed once in minimum essential medium + 0.1% BSA. Cells were then fixed with 4% paraformaldehyde, washed three times with PBS, and blocked with blocking buffer (3% dry milk in 50 mM Tris-HCl, pH 7.5). Hereafter, cells were incubated with the primary monoclonal mouse anti-HA antibody (Sigma-Aldrich) diluted in blocking buffer at 1:400 for 1 h at room temperature followed by three washes and a 1-h incubation with secondary antibody (1:1000, goat anti-mouse conjugated to horseradish peroxidase, Sigma-Aldrich) in blocking buffer. After three final washes, the secondary antibody was detected and quantified after adding the colorimetric horseradish peroxidase substrate 3,3′,5,5′-tetramethylbenzidine (Sigma-Aldrich). When adequate color change was reached, the reaction was terminated by the addition of 0.5 M H_2SO_4. Samples were then transferred to a 96-well plate, and colorimetric readings were obtained at optical density of 450 nM on a Tecan Sunrise absorbance reader (Tecan, Maennedorf, Switzerland). All experiments were performed in triplicate.

ERK1/2 phosphorylation assays

FFA1-eYFP mediated activation of ERK 1/2 was assessed using the SureFire ERK1/2 AlphaScreen assay from Perkin Elmer (Buckinghamshire, UK) and read on a BMG Labtech PheraSTAR FS plate reader (Buckinghamshire, UK), as described previously[4]. Briefly, HEK293 Flp-In™ T-REx cells expressing inducible FFA1-eYFP were seeded in poly-D-lysine coated 96-well culture plates at 40,000 cells per well and treated with 0.5 ug/ml doxycycline to induce receptor expression as required. The night before assay, appropriate wells were incubated with 20 ng/ml Pertussis toxin, and all cells were serum starved in cell culture medium lacking dialyzed fetal bovine serum for 2 hours on the day of assay. After 30 min of agonist stimulation, ERK1/2 activation was terminated by aspiration of assay medium and immediate addition of lysis buffer provided with the kit. Phosphorylated ERK1/2 was then quantified according to manufacturer's instructions.

REFERENCES SUPPLEMENTAL MATERIAL (KOSTENIS)

1. Wise, A. et al. Molecular identification of high and low affinity receptors for nicotinic acid. *J Biol Chem* **278**, 9869-9874 (2003).
2. Hosoi, T. et al. Identification of a novel human eicosanoid receptor coupled to G(i/o). *J Biol Chem* **277**, 31459-31465 (2002).
3. Brown, A.J. et al. The Orphan G protein-coupled receptors GPR41 and GPR43 are activated by propionate and other short chain carboxylic acids. *J Biol Chem* **278**, 11312-11319 (2003).
4. Smith, N.J. et al. The mode of binding of thiazolidinedione ligands at free fatty acid receptor 1. *J Biol Chem* **284**, 17527-17539 (2009).